COMPARISON OF TWO PROXIMAL SPLITTING ALGORITHMS FOR SOLVING MULTILABEL DISPARITY ESTIMATION PROBLEMS

Sonja Hiltunen[1], *Jean-Christophe Pesquet*[2] *and Béatrice Pesquet-Popescu*[3]

(1) Kungliga Tekniska Högskolan, Sound and Image Processing,
KTH Main Campus, Osquldas väg 10, 11428 Stockholm, Sweden.
(2) Université Paris-Est, LIGM and UMR-CNRS 8049,
5, Bd Descartes, Champs sur Marne, 77454 Marne la Vallée Cédex 2, France.
(3) Telecom ParisTech, Signal and Image Processing Department,
46, rue Barrault, 75634 Paris Cédex 13, France

Email: sonjahi@kth.se,pesquet@univ-mlv.fr,beatrice.pesquet@telecom-paristech.fr

ABSTRACT

Disparity estimation constitutes an active research area in stereo vision, and in recent years, global estimation methods aiming at minimizing an energy function over the whole image have gained a lot of attention. To overcome the difficulties raised by the nonconvexity of the minimized criterion, convex relaxations have been proposed by several authors. In this paper, the global energy function is made convex by quantizing the disparity map and converting it into a set of binary fields. It is shown that the problem can then be efficiently solved by parallel proximal splitting approaches. A primal algorithm and a primal-dual one are proposed and compared based on numerical tests.

***Index Terms*—** stereo vision, convex optimization, disparity estimation, total variation, segmentation.

1. INTRODUCTION

There has been recently a growing interest for convex relaxations of challenging variational problems arising in signal/image processing and computer vision. In this paper, we will be interested in variational formulations of disparity estimation problems. Recall that a stereo vision system captures two views of the same scene taken from slightly different angles. An important task in this context is stereo correspondence, the problem of finding the pixels in both images which correspond to the projections of the same 3D point. Global convex relaxation methods for depth estimation have been developed in recent years. They can be divided into algorithms operating on a discrete set of values, and techniques modeling directly the parameter space as being continuous.

The algorithms introduced in [1, 2] are continuous global variational techniques using non-smooth convex analysis tools. Due to the weak assumptions required by proximal methods, the algorithm in [2] provides flexibility in defining the energy function: it can use any convex data fidelity term with a well-defined proximity operator and any convex constraint with a closed-form projection. A drawback of this method is that it makes the globally optimized function convex by performing a first-order Taylor expansion, which in turn makes the approach dependent on an initial disparity estimate.

Alternative solutions can be obtained by formulating the disparity estimation problem as a combinatorial optimization one. Relaxations based on linear programming [3] or more sophisticated convex optimization approaches [4] have been proposed. In [4] (see also [5]), the energy function is made convex by converting the disparity field into a set of binary fields and relaxing the associated binary constraints. The energy function is thus convexified without making the result of the minimization process dependent on the initial disparity estimate. However, as the disparity estimates are constrained to belong to a finite set of quantization levels, an accurate estimation of the disparity map requires a fine enough quantization to be performed, so making the choice of efficient large-scale convex optimization algorithms mandatory.

Following this approach, we take advantage of recent advances in convex optimization methods [6] to develop algorithms allowing us to solve the convex relaxation formulation of multilabel disparity estimation problems. Two proximal methods are compared : a primal approach and a primal-dual one. The performances of these techniques are also evaluated with respect to another convex relaxation approach.

The paper is organized as follows: Section 2 introduces the considered relaxed formulation for disparity estimation. Then, in Section 3, a splitting approach for addressing the related optimization problem is described, together with the derivation of the required proximal operators. In Section 4, the implementation of the two proposed parallel proximal splitting algorithms are explained in detail. Section 5 presents the results of both algorithms. Section 6 concludes the present work.

2. CONVEX FORMULATION

We aim at solving the disparity estimation problem, based on the following global error measure

$$J(u) = \sum_{(x,y)\in\mathcal{D}\setminus\mathcal{O}} \phi\big(I_L(x,y), I_R(x-u(x,y),y)\big) \tag{1}$$

where u is the disparity field to be estimated, I_L designates the left image, I_R the right one, $\mathcal{D} = \{1,\dots,N\}\times\{1,\dots,M\}$ is the considered discrete image domain and $\mathcal{O}$ the occluded areas. $\phi : \mathbb{R}^2 \to]-\infty,+\infty]$ can be basically any similarity measure. We further assume that the disparity values are quantized over $Q+1$ levels, taking values $\{r_0,\dots,r_Q\}$ where $r_0 < \dots < r_Q$. Following the approach in [4], we introduce the binary fields $\theta_1,\dots,\theta_Q$ such that, for every $i \in \{1,\dots,Q\}$ and every $(x,y)\in\mathcal{D}$,

$$\theta_i(x,y) = \begin{cases} 1 & \text{if } u(x,y) \geq r_i \\ 0 & \text{otherwise.} \end{cases} \tag{2}$$

It can be noticed that the multivariate image $\theta = (\theta_1,\dots,\theta_Q)$ belongs to the set:

$$\mathcal{B} = \{\theta = (\theta_1,\dots,\theta_Q) \in (\{0,1\}^{N\times M})^Q \mid \big(\forall (x,y)\in\mathcal{D}\big)\; 1 \geq \theta_1(x,y) \geq \dots \geq \theta_Q(x,y) \geq 0\}.$$

More precisely, there exists a bijection between the set of disparity fields $u \in \{r_0,\dots,r_Q\}^{N\times M}$ and the set of multivariate images θ as defined above. We have then:

$$u(x,y) = r_0 + \sum_{i=1}^{Q}(r_i - r_{i-1})\theta_i(x,y). \tag{3}$$

The estimation of the quantized disparity u is thus equivalent to finding the associated multivariate binary field $\theta\in\mathcal{B}$. It can be further observed that the global error measure can be re-expressed as a linear function of θ as follows:

$$\widetilde{J}(\theta) = \sum_{i=0}^{Q}\sum_{(x,y)\in\mathcal{D}\setminus\mathcal{O}} \phi\big(I_L(x,y), I_R(x-r_i,y)\big) \times \big(\theta_i(x,y) - \theta_{i+1}(x,y)\big) \tag{4}$$

by setting $\theta_0 \equiv 1$ and $\theta_{Q+1} \equiv 0$. Disparity estimation is an ill-posed problem due in particular to the presence of uniform areas and occlusions. A classical solution to overcome this problem is to resort to a regularization of the problems by minimizing the criterion $J+\rho$, where ρ is some appropriate smoothness measure. As a disparity field often looks like a piecewise constant image with sharp contours, an appropriate smoothness measure is the total variation: $\rho = \mu\,\mathrm{tv}$, where $\mu > 0$ is the so-called regularization hyperparameter. Various expressions of the total variation can be found in the discrete case. For example, one can use the classical discrete form of the isotropic total variation. Following [4], the total variation regularized problem can be formulated as the following optimization problem:

$$\underset{\theta\in\mathcal{B}}{\text{minimize}}\;\; \widetilde{J}(\theta) + \mu\sum_{i=1}^{Q}(r_i - r_{i-1})\mathrm{tv}(\theta_i). \tag{5}$$

Although $\widetilde{J}$ and tv are convex functions, the problem is nonconvex due to the nonconvexity of the set $\mathcal{B}$. As demonstrated in [4], the following convex relaxation of the optimization problem can however be employed:

$$\underset{\theta\in\mathcal{R}}{\text{minimize}}\;\; \widetilde{J}(\theta) + \mu\sum_{i=1}^{Q}(r_i - r_{i-1})\mathrm{tv}(\theta_i) \tag{6}$$

where $\mathcal{R}$ is the convex hull of $\mathcal{B}$, that is

$$\mathcal{R} = \{\theta = (\theta_1,\dots,\theta_Q) \in ([0,1]^{N\times M})^Q \mid \big(\forall (x,y)\in\mathcal{D}\big)\; 1 \geq \theta_1(x,y) \geq \dots \geq \theta_Q(x,y) \geq 0\}.$$

Note that, since $\widetilde{J}$ is a continuous convex function defined on $(\mathbb{R}^{N\times M})^Q$, tv is a continuous convex function defined on $\mathbb{R}^{N\times M}$, and $\mathcal{R}$ is a compact convex set of $(\mathbb{R}^{N\times M})^Q$, the existence of a solution to Problem (6) is secured by standard results in convex optimization. The uniqueness of a solution is not however guaranteed.

3. PROXIMAL SOLUTIONS

3.1. Problem splitting

In order to efficiently solve Problem (6), we will need to introduce auxiliary variables and functions. Let us first define the following linear function: $\big(\forall\theta\in(\mathbb{R}^{N\times M})^Q\big)$

$$\begin{aligned} f_1(\theta) &= \widetilde{J}(\theta) - \sum_{(x,y)\in\mathcal{D}\setminus\mathcal{O}} \phi\big(I_L(x,y), I_R(x-r_0,y)\big) \\ &= \sum_{i=1}^{Q}\sum_{(x,y)\in\mathcal{D}} \varphi_i(x,y)\theta_i(x,y) = \langle\varphi \mid \theta\rangle \end{aligned}$$

where $\langle\cdot\mid\cdot\rangle$ designates the standard Euclidean inner product, $\varphi = (\varphi_1,\dots,\varphi_Q)\in(\mathbb{R}^{N\times M})^Q$, and, for every $i\in\{1,\dots,Q\}$ and $(x,y)\in\mathcal{D}$,

$$\varphi_i(x,y) = \begin{cases} \phi\big(I_L(x,y), I_R(x-r_i,y)\big) & \\ -\phi\big(I_L(x,y), I_R(x-r_{i-1},y)\big) & \text{if } (x,y)\notin\mathcal{O} \\ 0 & \text{otherwise.} \end{cases} \tag{7}$$

Let us now consider the following expression of the discrete total variation regularization term: $\big(\forall\theta\in(\mathbb{R}^{N\times M})^Q\big)$ $\widetilde{\rho}(\theta) =$

$f_2(D\theta)$. In the above expression, D is the linear operator from $(\mathbb{R}^{N\times M})^Q$ to $(\mathbb{R}^{N\times M})^{2Q}$ given by

$$D = \begin{bmatrix} D_1 & 0 & \dots & & 0 \\ D_2 & 0 & & & \vdots \\ 0 & D_1 & & & \\ 0 & D_2 & & & \vdots \\ \vdots & \vdots & & & 0 \\ 0 & 0 & & 0 & D_1 \\ 0 & 0 & \dots & 0 & D_2 \end{bmatrix} \tag{8}$$

where D_1 and D_2 are the spatial gradient operators operating in the horizontal/vertical directions, which will be periodized for simplicity sake. These operators correspond to 2D filters with frequency responses $1 - \exp(-2\pi\imath\nu_1)$ and $1 - \exp(-2\pi\imath\nu_2)$, where (ν_1, ν_2) are the 2D horizontal/vertical frequency variables. In addition, $f_2 \colon (\mathbb{R}^{N\times M})^{2Q} \to \mathbb{R}$ is the convex function which, in the isotropic case, takes the form:

$$\begin{aligned} &\big(\forall \delta = (\delta_{1,1}, \delta_{1,2}, \dots, \delta_{Q,1}, \delta_{Q,2}) \in (\mathbb{R}^{N\times M})^{2Q}\big) \\ &f_2(\delta) = \mu \sum_{i=1}^{Q} (r_i - r_{i-1}) \\ &\qquad \times \sum_{x=1}^{N}\sum_{y=1}^{M} \sqrt{\big(\delta_{i,1}(x,y)\big)^2 + \big(\delta_{i,2}(x,y)\big)^2}. \end{aligned} \tag{9}$$

To take into account the constraint set $\mathcal{R}$ we will also introduce the convex sets $\mathcal{C}_1 = ([0,1]^{N\times M})^Q$ and $\mathcal{C}_2 = ([0,+\infty[^{N\times M})^{Q-1}$. We have then: $\theta \in \mathcal{R} \Leftrightarrow \big(\theta \in \mathcal{C}_1 \text{ and } L\theta \in \mathcal{C}_2\big)$, where $L \colon (\mathbb{R}^{N\times M})^Q \to (\mathbb{R}^{N\times M})^{Q-1}$ is the linear operator defined as: $(\forall \theta \in (\mathbb{R}^{N\times M})^Q)\ L\theta = (\zeta_1, \dots, \zeta_{Q-1})$ and, for every $(x,y) \in \mathcal{D}$,

$$\begin{bmatrix} \zeta_1(x,y) \\ \vdots \\ \zeta_{Q-1}(x,y) \end{bmatrix} = \boldsymbol{L} \begin{bmatrix} \theta_1(x,y) \\ \vdots \\ \theta_Q(x,y) \end{bmatrix} \tag{10}$$

with

$$\boldsymbol{L} = \begin{bmatrix} 1 & -1 & 0 & \dots & \dots & 0 \\ 0 & 1 & -1 & \ddots & & \vdots \\ \vdots & \ddots & \ddots & \ddots & \ddots & \vdots \\ \vdots & & \ddots & \ddots & \ddots & 0 \\ 0 & \dots & \dots & 0 & 1 & -1 \end{bmatrix} \in \mathbb{R}^{(Q-1)\times Q}. \tag{11}$$

Altogether, the above considerations show that Problem (6) is equivalent to

$$\underset{\theta \in (\mathbb{R}^{N\times M})^Q}{\text{minimize}} \ f_1(\theta) + f_2(D\theta) + \iota_{\mathcal{C}_1}(\theta) + \iota_{\mathcal{C}_2}(L\theta) \tag{12}$$

where $\iota_{\mathcal{C}_1}$ and $\iota_{\mathcal{C}_2}$ are the indicator functions of the closed convex sets $\mathcal{C}_1$ and $\mathcal{C}_2$.

Based on the above reformulation, different proximal implementations can be thought of. In particular, a primal algorithm such as PPXA+ [7] can be employed or primal-dual solutions [8, 9] can be applied.

3.2. Proximity operators

For being able to apply proximal algorithms, we need to compute the proximity operators of the different functions involved in the previous section. Since the proximity operator of a closed convex set $\mathcal{C}$ of a Hilbert space reduces to the projection $\mathsf{P}_{\mathcal{C}}$ onto this set, the proximity operators of $\iota_{\mathcal{C}_1}$ and $\iota_{\mathcal{C}_2}$ in (12) are easy to compute. Since f_1 is a linear function, it can be further deduced from standard properties of the proximity operator [6] that the proximity operator of $\gamma f_1 + \iota_{\mathcal{C}_1}$ with $\gamma \in\,]0, +\infty[$ is given by $\mathrm{prox}_{\gamma f_1 + \iota_{\mathcal{C}_1}} = \mathsf{P}_{\mathcal{C}_1}(\cdot - \gamma\varphi)$. Finally, the proximity operator of γf_2 with $\gamma \in\,]0, +\infty[$ follows from existing results [10]. Note that, in general, there does not exist closed form expressions for the proximity operator of the composition of a convex function and a linear operator, which is one of the difficulties we will have to address in the choice of the optimization algorithm.

4. ALGORITHMS

4.1. PPXA+

The application to Problem (12) of the extension of the Parallel Proximal Algorithm (PPXA [10]) which was proposed in [7] leads to the following iterative algorithm:

$$\begin{array}{l} \text{Initialization} \\ \left\lfloor \begin{array}{l} (\omega_1, \omega_2, \omega_3) \in\,]0, +\infty[^3,\ \lambda \in]0, 2[\\ t_1^{(0)} \in (\mathbb{R}^{N\times M})^Q,\ t_2^{(0)} \in (\mathbb{R}^{N\times M})^{2Q}, \\ t_3^{(0)} \in (\mathbb{R}^{N\times M})^{Q-1} \\ \theta^{(0)} = (\omega_1 \,\mathrm{Id} + \omega_2 D^* D + \omega_3 L^* L)^{-1} \\ \qquad \times (\omega_1 t_1^{(0)} + \omega_2 D^* t_2^{(0)} + \omega_3 L^* t_3^{(0)}) \end{array} \right. \\ \text{For } n = 0, 1, \dots \\ \left\lfloor \begin{array}{l} p_1^{(n)} = \mathsf{P}_{\mathcal{C}_1}(t_1^{(n)} - \omega_1^{-1}\varphi) \\ p_2^{(n)} = \mathrm{prox}_{\frac{f_2}{\omega_2}}(t_2^{(n)}) \\ p_3^{(n)} = \mathsf{P}_{\mathcal{C}_2}(t_3^{(n)}) \\ c^{(n)} = (\omega_1 \,\mathrm{Id} + \omega_2 D^* D + \omega_3 L^* L)^{-1} \\ \qquad \times (\omega_1 p_1^{(n)} + \omega_2 D^* p_2^{(n)} + \omega_3 L^* p_3^{(n)}) \\ t_1^{(n+1)} = t_1^{(n)} + \lambda(2c^{(n)} - \theta^{(n)} - p_1^{(n)}) \\ t_2^{(n+1)} = t_2^{(n)} + \lambda\big(D(2c^{(n)} - \theta^{(n)}) - p_2^{(n)}\big) \\ t_3^{(n+1)} = t_3^{(n)} + \lambda\big(L(2c^{(n)} - \theta^{(n)}) - p_3^{(n)}\big) \\ \theta^{(n+1)} = \theta^{(n)} + \lambda(c^{(n)} - \theta^{(n)}). \end{array} \right. \end{array} \tag{13}$$

Hereabove ω_1, ω_2, ω_3 and λ are parameters which have to be chosen experimentally. ω_1, ω_2 and ω_3 can be viewed as weighting factors in the combination of the proximity operators, whereas λ is a relaxation parameter. The expressions of $\mathsf{P}_{\mathcal{C}_1}$, $\mathrm{prox}_{\frac{f_2}{\omega_2}}$, and $\mathsf{P}_{\mathcal{C}_2}$ are provided in Section 3.2. D^* and L^*

designate the adjoint operators of D and L. The main difficulty in the implementation of the algorithm lies in the inversion of $\omega_1 \operatorname{Id} + \omega_2 D^* D + \omega_3 L^* L$. It can be seen that this operator corresponds to a 2D MIMO (Multi-Input Multi-Output) filter whose multivariate frequency response is $\boldsymbol{S}(\nu_1, \nu_2) = G(\nu_1, \nu_2)\boldsymbol{I} + \omega_3 \boldsymbol{L}^\top \boldsymbol{L} \in \mathbb{R}^{Q\times Q}$, where $G(\nu_1, \nu_2)$ is the following frequency response of an invertible SISO filter:

$$G(\nu_1, \nu_2) = \omega_1 + \omega_2(|1-\exp(2\pi\imath\nu_1)|^2 + |1-\exp(2\pi\imath\nu_2)|^2). \tag{14}$$

Hence, $(\omega_1 \operatorname{Id} + \omega_2 D^* D + \omega_3 L^* L)^{-1}$ corresponds to the 2D MIMO filter with frequency response $(\boldsymbol{S}(\nu_1, \nu_2))^{-1}$. The computations can be efficiently performed by resorting to the use of 2D Fast Fourier Transforms.

Proposition 4.1 in [7] shows that the sequences $(p_1^{(n)})_{n\in\mathbb{N}}$, $(c^{(n)})_{n\in\mathbb{N}}$ and $(\theta^{(n)})_{n\in\mathbb{N}}$ generated by Algorithm (13) converge to a solution $\overline{\theta}$ to Problem (6).

4.2. M+S FBF algorithm

Alternatively, we propose to employ the following Monotone+Skew Forward-Backward-Forward algorithm The main advantage of this primal-dual parallel proximal algorithm is that it does not to require any operator inversion.

$$
\begin{array}{l}
\text{Initialization}\\
\left\lfloor
\begin{array}{l}
\gamma \in]0, +\infty[\\
v_1^{(0)} \in (\mathbb{R}^{N\times M})^Q, v_2^{(0)} \in (\mathbb{R}^{N\times M})^Q, v_3^{(0)} \in (\mathbb{R}^{N\times M})^Q\\
t_1^{(0)} \in (\mathbb{R}^{N\times M})^Q, t_2^{(0)} \in (\mathbb{R}^{N\times M})^{2Q}, t_3^{(0)} \in (\mathbb{R}^{N\times M})^{Q-1}
\end{array}
\right.\\
\text{For } n = 0, 1, \ldots\\
\left\lfloor
\begin{array}{l}
\theta^{(n)} = \frac{1}{3}(v_1^{(n)} + v_2^{(n)} + v_3^{(n)})\\
\widehat{v}_1^{(n)} = v_1^{(n)} - \gamma t_1^{(n)}\\
\widehat{v}_2^{(n)} = v_2^{(n)} - \gamma D^* t_2^{(n)}\\
\widehat{v}_3^{(n)} = v_3^{(n)} - \gamma L^* t_3^{(n)}\\
\widehat{t}_1^{(n)} = t_1^{(n)} + \gamma v_1^{(n)}\\
\widehat{t}_2^{(n)} = t_2^{(n)} + \gamma D v_2^{(n)}\\
\widehat{t}_3^{(n)} = t_3^{(n)} + \gamma L v_3^{(n)}\\
q^{(n)} = \frac{1}{3}(\widehat{v}_1^{(n)} + \widehat{v}_2^{(n)} + \widehat{v}_3^{(n)})\\
p_1^{(n)} = \widehat{t}_1^{(n)} - \gamma \mathsf{P}_{C_1}(\gamma^{-1}(\widehat{t}_1^{(n)} - \varphi))\\
p_2^{(n)} = \widehat{t}_2^{(n)} - \gamma \operatorname{prox}_{\gamma^{-1} f_2}(\gamma^{-1}\widehat{t}_2^{(n)})\\
p_3^{(n)} = \widehat{t}_3^{(n)} - \gamma \mathsf{P}_{C_2}(\gamma^{-1}\widehat{t}_3^{(n)})\\
\widetilde{v}_1^{(n)} = q^{(n)} - \gamma p_1^{(n)}\\
\widetilde{v}_2^{(n)} = q^{(n)} - \gamma D^* p_2^{(n)}\\
\widetilde{v}_3^{(n)} = q^{(n)} - \gamma L^* p_3^{(n)}\\
\widetilde{t}_1^{(n)} = p_1^{(n)} + \gamma q^{(n)}\\
\widetilde{t}_2^{(n)} = p_2^{(n)} + \gamma D q^{(n)}\\
\widetilde{t}_3^{(n)} = p_3^{(n)} + \gamma L q^{(n)}\\
\text{For } j = 1, 2, 3\\
\left\lfloor
\begin{array}{l}
v_j^{(n+1)} = v_j^{(n)} - \widehat{v}_j^{(n)} + \widetilde{v}_j^{(n)}\\
t_j^{(n+1)} = t_j^{(n)} - \widehat{t}_j^{(n)} + \widetilde{t}_j^{(n)}.
\end{array}
\right.
\end{array}
\right.
\end{array}
\tag{15}
$$

According to [9, Prop.4.4], if $\gamma \in [\varepsilon, (1-\varepsilon)/\beta]$ where $\beta = \max(1, \|D\|, \|L\|)$ and $\varepsilon \in]0, 1/(\beta+1)[$, then the sequence $(\theta^{(n)})_{n\in\mathbb{N}}$ generated by Algorithm (15) converges to a solution $\overline{\theta}$ to Problem (6). In practice, to accelerate the convergence, the step size γ has to be chosen as large as possible (for example, $\epsilon = 0.01/(\beta+1)$ and $\gamma = (1-\varepsilon)/\beta$). Due to the forms of operators L and D, we have $\|L\| = \|\boldsymbol{L}\| \leq 2$ and $\|D\| = 2\sqrt{2}$, so leading to $\beta = 2\sqrt{2}$.

5. SIMULATION RESULTS

The experiments have been performed on test images with known ground truth disparity maps. For the computation of φ from (7) for non-integer pixel values, the fields have been bilinearly interpolated. In the provided results, the data term used is the mean absolute difference. The accuracy of the results is measured in PSNR, defined as $\text{PSNR} = 10\log_{10}\left(u_{\max}^2/\text{MSE}\right)$, where $u_{\max}$ is the maximum disparity value of the ground truth disparity image, and

$$\text{MSE} = \frac{1}{|\mathcal{D}|}\sum_{(x,y)\in\mathcal{D}} |u_{\text{ground truth}} - u_{\text{algorithm}}|^2. \tag{16}$$

It should be noticed that since the algorithms aim at minimizing Criterion (6), they do not explicitly maximize the PSNR, but getting a high PSNR is a side effect.

The regularization hyperparameter μ affects the smoothness of the obtained disparity maps. If it is too small, the resulting disparity map looks grainy. As it increases, the resulting disparity map is smoothed out, while blurring the details. This parameter has been chosen experimentally in order to maximize the PSNR. In the results, $\mu = 1.1$ for 'Aloe', $\mu = 9$ for 'Cones' and $\mu = 3$ for 'Saw' and 'Corridor'. Algorithms for automatically determining μ could also be employed at the expense of a higher computational cost.

Figure 1 illustrates the convergence of the two algorithms as a function of running time for a Matlab implementation on a single core architecture. They are obtained for $\omega_1 = 1$, $\omega_2 = 3$ and $\omega_3 = 2$, $\lambda = 1.8$ and $\gamma = 0.35$. Even better results could be obtained by choosing optimal parameters for different step size values. Although PPXA+ converges faster, it has a disadvantage of requiring a large amount of memory to perform the MIMO-filtering and if applicable, storing the filter. For a large number of quantization levels (about more than 60), this makes it less feasible to perform the computations in Matlab.

Furthermore, it should be determined when it is appropriate to threshold the optimized disparity field so that it at least approximately coincides with a solution to (5). If the algorithms were run for an infinite amount of time and for a continuous-space model, the disparity map given by minimizing (6) would be asymptotically discrete valued. In a real context, the resulting fields can be thresholded if the approximation of the disparity is accurate enough. The choice of thresholding is not computationally demanding; first an unthresholded disparity map is computed, then the thresholding which results in the highest PSNR is chosen.

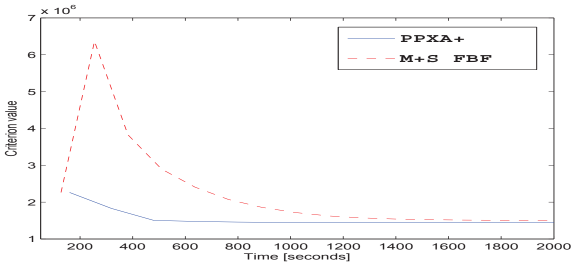

(a) Cones

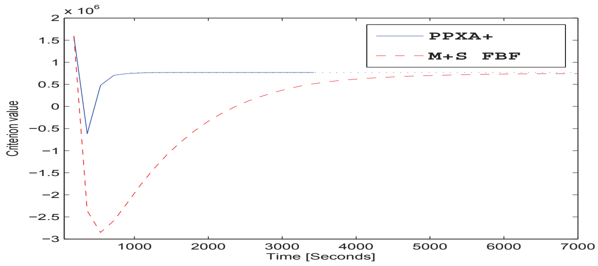

(b) Aloe

Fig. 1. Comparison of convergence for the two algorithms.

Image	Aloe	Cones	Saw	Corridor
Proposed algorithm	23.41	24.09	24.32	28.79
Algorithm [2]	21.12	23.97	23.08	25.72

Table 1. PSNR of the proposed algorithms compared with [2]

Experimental results for PPXA+ show that the PSNR is relatively stable after 200 iterations for the test images, and only a small gain is attainable afterwards.

Table 2 compares the resulting PSNR values with those provided by another algorithm, the one in [2], where the initialization has been performed by block matching. Figure 2 displays the disparity maps obtained with the proposed algorithms.

6. CONCLUSION

We have presented a new convex relaxation approach for disparity estimation based on proximal optimization algorithms. The main advantage of this approach is that the algorithm is not sensitive to the initial disparity map. It has also been shown that for a reasonable number of disparity quantization levels, PPXA+ outperforms the M+S FBF algorithm in terms of convergence speed. It is worth mentioning that the proposed methods could be applied to other multilabel segmentation problems.

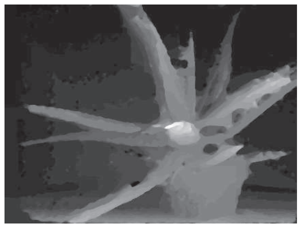

(a) Aloe, 29 quantization levels

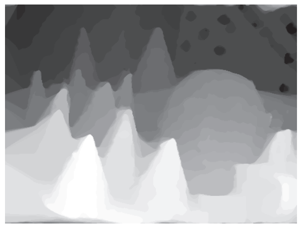

(b) Cones, 51 quantization levels

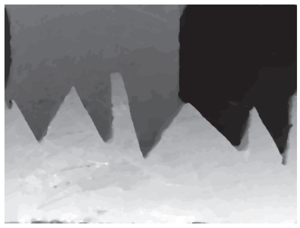

(c) Saw, 43 quantization levels

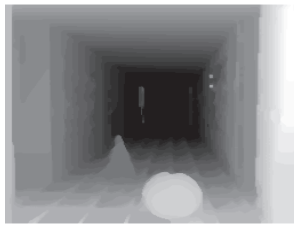

(d) Corridor, 37 quantization levels

Fig. 2. Disparity maps for the proposed algorithms.

7. REFERENCES

[1] W. Miled, J.-C. Pesquet, and M. Parent, "A convex optimization approach for depth estimation under illumination variation," *IEEE Trans. Image Process.*, vol. 18, pp. 813–830, Apr. 2009.

[2] M. El-Gheche, J-C Pesquet, J. Farah, M. Kaaniche, and B. Pesquet-Popescu, "Proximal splitting methods for depth estimation," in *Proc. Int. Conf. Acoust. Speech, Signal Processing*, Prague, Czech Republic, May 22-27 2011, pp. 853–856.

[3] N. Komodakis, N. Paragios, and G. Tziritas, "MRF energy minimization and beyond via dual decomposition," *IEEE Trans. Pattern Anal.*, vol. 33, no. 3, pp. 531–552, May 2011.

[4] D. Cremers, P. Thomas, K. Kolev, and A. Chambolle, "Convex relaxation techniques for segmentation, stereo and multiview reconstruction," in *Markov Random Fields for Vision and Image Processing*, A. Blake, P. Kohli, and C. Rother, Eds. The MIT Press, Boston, 2011.

[5] T. Chan, S. Esedoglu, and M. Nikolova., "Algorithms for finding global minimizers of image segmentation and denoising models," *SIAM Journal of Applied Mathematics*, vol. 66, pp. 1632–1648, 2006.

[6] P. L. Combettes and J.-C. Pesquet, "Proximal splitting methods in signal processing," in *Fixed-Point Algorithms for Inverse Problems in Science and Engineering*, H. H. Bauschke, R. Burachik, P. L. Combettes, V. Elser, D. R. Luke, and H. Wolkowicz, Eds., pp. 185–212. Springer-Verlag, New York, 2011.

[7] J.-C. Pesquet and N. Pustelnik, "A parallel inertial proximal optimization method," *Pacific Journal of Optimization*, vol. 8, no. 2, pp. 273-305, Apr. 2012.

[8] A. Chambolle and T. Pock, "A first-order primal-dual algorithm for convex problems with applications to imaging," *J. Math. Imaging Vision*, vol. 40, no. 1, pp. 120–145, 2010.

[9] L. M. Briceño-Arias and P. L. Combettes, "A monotone + skew splitting model for composite monotone inclusions in duality," *SIAM J. Optim.*, vol. 21, no. 4, pp. 1230–1250, Oct. 2011.

[10] P. L. Combettes and J.-C. Pesquet, "A proximal decomposition method for solving convex variational inverse problems," *Inverse Problems*, vol. 24, 2008, 27 p., art. 065014.